

Determining the location of the tip of the red giant branch in old stellar populations: M33, Andromeda I and II

A. W. McConnachie,¹★ M. J. Irwin,¹ A. M. N. Ferguson,² R. A. Ibata,³
G. F. Lewis⁴ and N. Tanvir⁵

¹Institute of Astronomy, Madingley Road, Cambridge CB3 0HA

²Max-Planck-Institut für Astrophysik, Karl-Schwarzschild-Str. 1, Postfach 1317, D-85741 Garching, Germany

³Observatoire de Strasbourg, 11, rue de l'Université, F-67000, Strasbourg, France

⁴Institute of Astronomy, School of Physics, A29, University of Sydney, NSW 2006, Australia

⁵Physics, Astronomy and Mathematics Department, University of Hertfordshire, Hatfield AL10 9AB

Accepted 2004 January 16. Received 2004 January 16; in original form 2003 November 14

ABSTRACT

The absolute bolometric luminosity of the point of core helium ignition in old, metal-poor, red giant stars is of roughly constant magnitude, varying only very slightly with mass or metallicity. It can thus be used as a standard candle. Here, we review the main difficulties in measuring this location in any real data set and we develop an empirical approach to optimize it for tip of the red giant branch (TRGB) analysis. We go on to present a new algorithm for the identification of the TRGB in nearby metal-poor stellar systems. Our method uses a least-squares fit of a data adaptive slope to the luminosity function in 1-mag windows. This finds the region of the luminosity function that shows the most significant decline in star counts as we go to brighter magnitudes; the base of this decline is attributed as the location of the tip. This technique then allows for the determination of realistic uncertainties which reflect the quality of the luminosity function used, but which are typically ~ 0.02 mag rms + ~ 0.03 mag systematic, a significant improvement upon previous methods that have used the tip as a standard candle. Finally, we apply our technique to the Local Group spiral galaxy M33 and the dwarf galaxies Andromeda I and II, and derive distance modulii of 24.50 ± 0.06 mag (794 ± 23 kpc), 24.33 ± 0.07 mag (735 ± 23 kpc) and 24.05 ± 0.06 mag (645 ± 19 kpc) respectively. The result for M33 is in excellent agreement with the Cepheid distances to this galaxy, and makes the possibility of a significant amount of reddening in this object unlikely.

Key words: galaxies: general – Local Group – galaxies: stellar content.

1 INTRODUCTION

The accurate determination of distances in the Universe is a fundamental and difficult problem in astronomy. Parallax is the ideal method of distance determination as it is completely independent of the physical nature of the body of interest. However, this geometrical method can only be currently applied successfully in the nearby Galaxy because of limitations in the accuracy of the astrometry required. For systems external to this, we are forced to search for some standard candle – an object whose intrinsic brightness we think we know. Measurement of the apparent brightness can then, after correction for extinction effects, lead to an estimate of its actual distance. The most successful and reliable standard candle known in astrophysics is the Cepheid variable, whose well-studied period–

luminosity relation sets the foundation for the entire cosmological distance ladder (see, for example, Tanvir 1999).

One of the limitations of the Cepheid method is that it is confined to relatively massive Population I systems. In order to calculate distances to older, more metal-poor galaxies, some other standard candle is required. The tip of the red giant branch (TRGB) offers an ideal alternative for these systems. Physically, this stage in stellar evolution represents the point of the core helium flash. Here, the temperature of the degenerate, quasi-isothermal core is only dependent upon the properties of the thin H-burning shell around it, and this varies only very slightly with chemical abundance and surrounding mass. The TRGB is thus of roughly constant intrinsic brightness. Iben & Renzini (1983) realized that for low-mass, metal-poor stars ($[Fe/H] < -0.7$ dex) the TRGB varies by only ~ 0.1 mag for any star older than 2 Gyr. The absolute *I*-band magnitude is also found to be constant for these stars as absorption effects in the stellar atmosphere are minimal; however, for stars more metal-rich than this,

* E-mail: alan@ast.cam.ac.uk

molecular absorption causes the TRGB to appear dimmer in this band. A more recent study of the theoretical predictions concerning this stage in stellar evolution has been conducted by Salaris & Cassisi (1997) and a comparison with other distance indicators, such as Cepheid and RR Lyrae variables, was made. They found agreement between these methods at the level of ~ 0.1 mag.

Da Costa & Armandroff (1990) compared the brightest RGB stars in various globular clusters to the theoretical predictions for core helium ignition and found very good agreement between the two, with only a very weak dependency on metallicity. They were dealing with relatively sparse colour-magnitude diagrams (CMDs) however. A more recent study by Bellazzini, Ferraro & Pancino (2001) of the globular cluster ω Centauri came to similar conclusions. They obtained a value of the absolute I -band magnitude of the TRGB of -4.04 ± 0.12 mag. We shall later use this value in order to calculate the distance modulus to several galaxies (see Section 3.2 for a discussion of this result).

Several authors have used various techniques to derive TRGB distances. For example, Harris et al. (1998) used a model fitting technique to the luminosity function, although the most influential method to determine the location of the TRGB is due to Lee et al. (1993). Prior to this publication, estimates of the location of the TRGB had mostly been made by eye. Such a qualitative approach is, of course, not ideal as it is not reproducible. However, Lee, Freedman & Madore (1993) put the method on a quantitative basis by employing an edge detection algorithm. Essentially, an edge detection algorithm in this context compares neighbouring star counts and looks for the largest absolute change between neighbouring bins – in essence, it models the TRGB edge as a step. Specifically, Lee et al. used a zero-sum Sobel kernel $[-2, 0, 2]$ and convolved it with the binned luminosity function. The range over which this kernel is applied is defined by the sampling of the luminosity function. In practice, the output of this displays a maximum in the bin coincident with the largest absolute change in the counts. The mid-point of this bin was then assumed to be the magnitude of the TRGB. Typical uncertainties in this quantity were quoted as 0.1–0.2 mag.

Three years later, Sakai, Madore & Freedman (1996) adapted this method to make it independent of binning. They constructed a smoothed luminosity function $\wp(m)$ such that

$$\wp(m) = \sum_{i=1}^{N_*} \frac{1}{\sqrt{2\pi}\sigma_i} \exp\left[-\frac{(m_i - m)^2}{2\sigma_i^2}\right], \quad (1)$$

where m_i and σ_i are the magnitude and photometric error of the i th star from a sample of N_* . In the limit of large N_* , the result can be thought of as a luminosity probability distribution. Hereafter, we adopt the abbreviation LPD for this function, to distinguish it from the binned luminosity function. Sakai et al. then convolved this with a smoothed Sobel kernel, this time in the form of $[-2, -1, 0, 1, 2]$ – this kernel is less sensitive to spikes due to Poisson noise than the previously used one, as it allows for some smoothing of the luminosity function over a small range. This allowed them to find the position of the TRGB, as they had defined it, to within an uncertainty of ~ 0.1 mag. More recently, Mendez et al. (2002) have refined this method further, and they have also used it in conjunction with a maximum likelihood method. This involved modelling the RGB in the luminosity function as a truncated power law and attributing the TRGB as the location at which the power law is truncated. We believe that such a technique is a significant improvement over the Sobel edge detection algorithms and it offers many advantages; for example, it is much more stable against noise effects. However, a step model (an abrupt cut-off in number counts) is still implicitly assumed as the intrinsic shape of the TRGB in their analysis.

It is not clear that an edge detection algorithm, or any method that assumes a step in the luminosity function, is necessarily the best approach to this problem, as there is no a priori reason why the luminosity function at the location of the tip should be a simple step function. It may equally well be a slope, or a parabola, or something else – the exact shape of the luminosity function at the TRGB edge is currently unknown. We note that Zoccali & Piotto (2000) show that the bright end of RGB luminosity function is well modelled by a simple power law, but there is no model that predicts the shape of the TRGB edge, although this doubtless depends upon the number of stars that contribute to the luminosity function. Generally, we might expect the number of stars to decrease gradually over a short magnitude range as we approach the tip from along the RGB. The luminosity function would then exhibit more of a slope at the TRGB; an abrupt change in the bright end of this slope would then be, by definition, the TRGB. The Sobel edge detection algorithm does not always produce a peak in such a situation (see, for example, fig. 1 of Madore & Freedman 1995). In practice, the resulting signal is not easy to detect over and above all the other random variations that the output of this procedure creates when dealing with all but the most idealized noise-free luminosity functions.

In Section 2 of this paper, we review the main difficulties with using the TRGB as a distance indicator. We then describe and test a new algorithm that we have created in order to measure the TRGB location. This algorithm is based upon a least-squares fitting procedure and makes fewer assumptions about the shape of the luminosity function at the TRGB, working equally well for situations where the TRGB is marked by a sudden or gradual rise in star counts. This data adaptive slope technique gives uncertainties in the distance modulus obtained typically of the order of ~ 0.05 mag, but most importantly reflects the quality of the luminosity function used. We also demonstrate an additional simple empirical heuristic scheme that allows a first pass estimate of this location to be made. In Section 3 we go on to apply our method to calculate the distances to the spiral galaxy M33 and the dwarf galaxies Andromeda I and II.

2 LOCATING THE TRGB

2.1 Data considerations

Finding the apparent magnitude of the TRGB in a satisfactory, quantitative manner has proved a challenge with several different techniques having been used in the literature. Madore & Freedman (1995) have already written an excellent review and used computer simulations to analyse the effects of these difficulties on the Sobel edge detection algorithm. They concluded that:

- (i) low signal-to-noise (S/N) can hide the location of the tip in a luminosity function or lead to the false identification of this point, with a jump due to noise possibly being attributed to the luminosity of core He ignition;
- (ii) bright asymptotic giant branch (AGB) stars can contaminate the luminosity function in the region of the tip, and may hide its true location;
- (iii) foreground stars masquerade as members of the stellar system and will contaminate the luminosity function.

Poisson noise is usually the dominant uncertainty in any luminosity function, and becomes a serious issue if we intend to try and measure a specific location defined by some discontinuity in star counts. Although the algorithm we describe later is less sensitive to Poisson noise than an edge detection algorithm, or such like, it is still not immune. The only way to overcome Poisson errors

successfully is to obtain photometry for more stars. As well as decreasing the resulting noise in a luminosity function, large star counts also ensure that the luminosity function we construct from our sample is as close to the underlying luminosity function of the population as possible. Therefore, the most luminous RGB stars are more likely to be at the point of core helium ignition – although we note that Crocker & Rood (1984) conducted Monte Carlo simulations which suggest that there is a large probability of observing a star close to the tip location even for a sample of relatively few RGB stars. Additionally, the effect of Malmquist bias on a well-sampled luminosity function is negligible.

Many previous TRGB distance studies have used *Hubble Space Telescope (HST)* Wide Field Planetary Camera 2 (WFPC2) data (e.g. Kim et al. 2002; Maíz-Apellániz et al. 2002). However, despite the superb resolution of the WFPC2, its relatively small field of view (FOV; an L-shaped 2.5×2.5 arcmin 2) may sometimes not allow for as large a number of bright RGB stars to be observed as is required for a relatively noise-free luminosity function suitable for TRGB analysis. Instead, wherever possible, to maximize the number of stars observed and to increase the reliability of the TRGB measurement, we advocate the use of ground-based wide field cameras, for example the Wide Field Camera on the Isaac Newton Telescope (INT; 0.29° FOV) or MEGACAM on the Canada–France–Hawaii Telescope (1° FOV). The accuracy of the technique that we introduce later is significantly improved if used on a well-defined luminosity function, although realistic error estimations are obtained regardless of the number of stars contributing to the measurement. In these situations however, we may need to concern ourselves with whether the luminosity function we create is representative of the underlying population.

Having maximized the number of stars with reliable photometry, we then want to increase the S/N for the resultant luminosity function. By signal we refer to RGB stars in the system of interest, and by noise we refer to everything else – AGB stars and foreground stars, in particular. The most obvious way to increase the fraction of RGB stars on the luminosity function is to take the luminosity function along the RGB only. This is most easily illustrated by looking at Fig. 8, which shows the CMD for And I & II. The luminosity function is only plotted for the stars bounded by the dotted lines. Their positions are determined by taking star counts in strips parallel to the RGB and placing the boundaries on either side of the maximum. The exact position or separation of the boundaries makes no difference to the derived value for the tip, as should be expected. All the other stars outside this area are ignored, as they contribute nothing to the RGB and would only act to hide the tip. Some bright AGB stars may still be present but their effect has been lessened. Further, as we demonstrate in Section 2.2.1, our technique for finding the RGB appears robust even with a significant AGB population.

Some foreground stars will have survived the cut that we have applied to our data and will be contaminating our RGB luminosity function. We cannot hope to identify foreground stars individually but with wide field data we are able to apply a statistical correction for them by using a luminosity function of a neighbouring region consisting only of foreground stars. Then, assuming that all the brighter stars in our fields of interest are foreground objects, we can use these to scale the reference luminosity function to our data if necessary.

Finally, we propose to use, in the same way as Sakai et al. (1996), the LPD given by equation (1) instead of the normal binned histogram. This makes the process independent of any binning considerations and yields a continuous function for the analysis, with the drawback that the error analysis becomes more complicated

than for a normal luminosity function. Taken as a whole, the above methodology creates clean LPDs optimized to measure the TRGB. Further specific discussion of our data is deferred until Section 3 after we have described the algorithm we are using to analyse LPDs for TRGB locations.

2.2 Least-squares fitting of an adaptive slope

The technique that we use to locate the TRGB involves finding the region on a LPD that shows the most significant decline in star counts. The base of this decline (slope) will be attributable to the TRGB. The main complication arises because of our lack of knowledge of the intrinsic shape of the LPD around the TRGB location, and what gradient best resembles the slope in this region. Fitting an optimum model to the LPD therefore implies a generalized least-squares fitting procedure. Note that the model we use is not defined over the full range of the LPD, as it is not our intention to model the LPD but to locate a specific point of the LPD. By making this our goal we minimize the assumptions that we are forced to make concerning the intrinsic shape of the LPD. We instead repeatedly look at the LPD through a window, and find the window in which the LPD is best fit as a simple slope function; that is, the region that, when coming from the faint end, demonstrates the most significant decline in star counts.

In least-squares fitting, we seek to find the values of model parameters which for independent errors minimize the function χ^2 , given by

$$\chi^2 = \sum_{i=1}^N \frac{(d_i - m_i)^2}{\sigma_i^2} \quad (2)$$

where d_i is the i th data point with an uncertainty σ_i , and m_i is the corresponding point in the model. Assuming the model chosen is a good one, then the best fit should produce a χ^2_{min} which is equal to the number of degrees of freedom. If we used a single model shape, then we would require only one parameter, τ , which would govern the x -axis offset between data and model. However, we do not want to specify the slope to be fitted, and so instead we use a family of templates, ϕ_s , where s is a parameter which governs the gradient of the template. In all, the template is defined over a 1-mag range, chosen empirically as the range that is generally sufficient to show the feature we are attempting to fit, while still allowing our model to be a reasonable approximation to the feature. Because this extends over a shorter x -axis range than the complete LPD, then the y -axis range of the data that we fit to changes with τ . We thus need to introduce two scaling parameters to deal with this; a vertical scalefactor $k_{\tau,s}$ and a ‘dc offset’ $a_{\tau,s}$. For any values of s and τ , the relationship between the actual model fitted, $m_{\tau,s}$, and the template, ϕ_s , is then

$$m_{\tau,s} = k_{\tau,s}\phi_s + a_{\tau,s} \quad (3)$$

and so we are left to minimize the expression

$$\chi^2(s, \tau, k, a) = \sum_{i=1}^N \frac{[d_{i+\tau} - (k_{\tau,s}\phi_{s,i} + a_{\tau,s})]^2}{\sigma_{i+\tau}^2} \quad (4)$$

where N now signifies the number of points defining our template ϕ_s , and we have defined τ such that it corresponds to an integer number of points in the data. Simple expressions for $a_{\tau,s}$ and $k_{\tau,s}$ may be derived by looking for the values which produce a minimum in χ^2 . By defining our templates such that $\sum_{i=1}^N \phi_{s,i} = 0$ and assuming a

constant error term we then find that

$$a_{\tau,s} = \frac{1}{N} \sum_{i=1}^N d_{i+\tau} \quad (5)$$

$$k_{\tau,s} = \frac{\sum_{i=1}^N d_{i+\tau} \phi_{s,i}}{\sum_{i=1}^N \phi_{s,i}^2}. \quad (6)$$

A constant error term is a reasonable approximation to the error distribution of the LPD, although its actual error distribution is complicated by the covariance of neighbouring regions. Every point on the LPD is a sum of contributions from every star and so a simple Poisson distribution is not valid. However, given that there are a large number of stars contributing to every point, then the central limit theorem implies that the errors can be well approximated by a constant error in this limit. A check of the validity of this approximation and its effect on the resulting uncertainties on the parameters is conducted with the M33 data in Section 3.3, and it is shown to be robust.

Our method is then as follows. We calculate $m_{\tau,s}$ for every value of τ and s by using the above prescription to calculate $k_{\tau,s}$ and $a_{\tau,s}$. We then conduct a simple least-squares fit of these models to the LPD, in 1-mag windows, and we find the values of s and τ that minimize $\chi^2(s, \tau k_{\tau,s}, a_{\tau,s})$. This then gives us the TRGB. Examination of the 1σ contours in the $\tau-s$ plane also gives us the uncertainty associated with this value. Because of the general nature of this fit, it is possible that at times the method may locate a feature that is nothing to do with the TRGB, but is perhaps a result of noise. However, such cases are rare for a well-sampled luminosity function, and are generally obvious. They are usually easily identified by visual inspection of the fit and appropriate constraints to the parameters can be applied if necessary.

2.2.1 Testing the data adaptive least-squares method

To test the robustness of the data adaptive slope method, we generated model CMDs that had a TRGB at twentieth magnitude, marked by a steady rise in star counts. Photometric noise was added by selecting a value from a Gaussian distribution with $\sigma = 0.02$ mag, the typical photometric uncertainty in our data at twentieth magnitude. It should be noted that we experimented with different error weightings but found that this had a negligible effect on our results, as in the range of interest around the TRGB the photometric error is well approximated by an error of 0.02 mag. We used a background of 8000 stars randomly distributed between nineteenth and twenty-third magnitude and populated a RGB between twentieth and twenty-third magnitude. Our method was then applied to this model CMD. Measuring the S/N as the ratio of the number of stars on the TRGB to those in the background (i.e. unwanted contaminants), the results as the S/N increases can be seen as the solid line in Fig. 1. For a S/N greater than approximately one, the measured position of the tip differs from the actual position by, at most, 0.02 mag. This nicely shows that the method is able to identify and fit the region of the TRGB to a high accuracy.

We ran a second set of tests which also included a large population of 1000 AGB stars randomly distributed between 19.5 and 20.5 mag, which will act to mask the tip (dashed line in Fig. 1). The behaviour of convergence with increasing S/N remains virtually unaltered for $S/N > 1$ even with a significant AGB population.

A third set of tests was conducted on the M33 data. In Section 3.2 we calculate that the TRGB for this galaxy lies at 20.54 mag (uncorrected for reddening), based upon some 20 000 stars contributing to

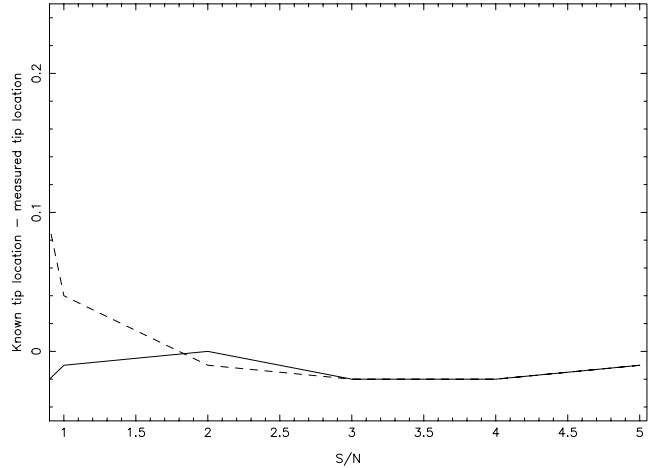


Figure 1. The convergence of the measured value of the tip with its known location as the S/N is increased (solid line). Here we define the S/N to be the ratio of the number of stars on the RGB to the background contaminants. The method is accurate even at low (~ 1) S/N. A second set of tests, which also considers the effect of an AGB population on the algorithm, shows comparable behaviour (dashed line), where this time the S/N is defined as the ratio of stars on the RGB to the sum of the background contaminants and the AGB population.

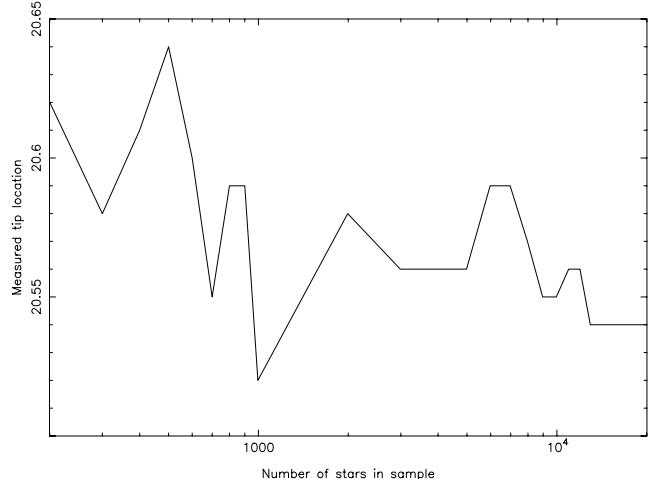


Figure 2. The variation of the measured location of the TRGB with star counts in M33. Despite the stellar sample size varying by two orders of magnitude, the peak-to-peak variation in the measured TRGB location is only 0.12 mag over the entire range.

the LPD. Fig. 2 shows how our measured value of the TRGB varies as we continually reduce this number. It is evident that, although the number of stars we use changes by two orders of magnitude, the peak-to-peak variation in the measured value of the tip is only 0.12 mag, decreasing to 0.05 mag when more than 2000 stars are considered. This demonstrates the stability of our technique over a very large range in star counts. There is also evidence of a trend such that, as we go to larger numbers, the measured location of the tip tends to brighter magnitudes. This is not to be unexpected because the larger sample of stars will ensure that the brightest RGB stars lie closer to the true tip location. This fact, and the decreasing scatter in the measured values as we go to larger numbers, shows that large number statistics are desirable for such a study.

2.3 Relative increases (heuristic)

Finally, we have developed a second, much simpler, method to estimate the location of the TRGB. This involves monitoring the relative increase in star counts between neighbouring bins in the foreground-corrected RGB luminosity function once the counts have exceeded a threshold level. Because we are only comparing neighbouring bins, then noise effects will affect us to a significant degree. To combat this, we (non-recursively) average each bin with its two immediate neighbours. The output should show a peak near the location of the TRGB. It is very useful to have such a simple method to provide an independent sanity-check of the results from the data adaptive least-squares technique.

3 DISTANCE DETERMINATIONS TO SOME LOCAL GROUP MEMBERS

3.1 Data

The Wide Field Camera on the 2.5-m INT consists of a four-chip EEV 4 K \times 2 K CCD mosaic camera that images $\simeq 0.29 \text{ deg}^2$ per exposure (Walton et al. 2001). Over the past three years we have been using this to conduct a survey of the halo and outer disc of our nearest neighbour, M31. This survey now extends out to over 55 kpc in projection from the centre of this galaxy. In 2002, we extended this project to include M33 which has now been mapped out to a radius of ~ 20 kpc. Even the early results of these surveys were startling, with the halo of M31 showing significant and unexpected substructure; the most spectacular of these being a massive tidal stream stretching out as far as we have surveyed (Ibata et al. 2001; Ferguson et al. 2002; McConnachie et al. 2003). As part of the M31 and M33 surveys we also took fields covering two of M31's dwarf spheroidal satellites, And I & II.

Images were taken in the equivalent of Johnson V (V') and Gunn i (i') bands. For both surveys, most of the data were taken in photometric conditions. The few non-photometric nights were calibrated using overlapping fields and the whole system was placed on a consistent scale using all of the field overlaps. The data for And I & II were deliberately acquired under photometric conditions. Exposure times of 800–1000 s per passband allowed us to reach $i' = 23.5$ mag and $V' = 24.5$ mag ($S/N \simeq 5$), and are sufficient to detect individual RGB stars to $M_{V'} \simeq 0$ mag and main-sequence stars to $M_{V'} \simeq -1$ mag at the distance of M31. Several fields taken in poorer conditions were reobserved and co-added as necessary to give an approximately uniform overall survey depth. For this paper, we have converted our data to the Johnson–Cousins system. The transformations employed are $I = i' - 0.101 \times (V-I)$ and $V = V' + 0.005 \times (V-I)$ and have been derived by comparison with observations of several Landolt standard fields.¹

All the on-target data plus calibration frames were processed using the standard INT Wide Field Survey (WFS) pipeline supplied by the Cambridge Astronomical Survey Unit (Irwin & Lewis 2001), which provides all the usual facilities for instrumental signature removal and astrometric and photometric calibration. Internal cross-calibration of the four CCDs is achieved at a level better than 1 per cent for each pointing. The overall derived photometric zero-points for the entire survey are good to the level of ± 2 per cent in both bands. Object classification uses the observed morphological structure on the CCDs but is vulnerable at faint magnitudes to distant

compact galaxies, which may be misclassified as stars. However, this does not seriously affect us here as we are generally dealing only with stars near the TRGB. For the purposes of this analysis, we concern ourselves only with those objects classified as stellar in both the V' and i' passbands.

As already discussed, the Galactic foreground stellar population should be subtracted from the data to minimize contaminants. In order to compensate for this population, we use a number of outer halo fields from our M31 survey for both M33 (where there is no suitable local reference field we can use) and And I (which is sufficiently close to M31 for the foregrounds to be similar). Although there is a low-level M31 halo population in these reference fields, the dominant population is galactic foreground stars, thus making them suitable as reference fields and allowing a statistical correction to be applied. The computed scaling using the brighter part of the CMDs compensates not only for the difference in area but also to first order the Galactic population gradient. For And II, we are able to apply a local foreground correction (see Section 3.5). In this study we typically find that the foreground contamination in the region of the TRGB is ~ 15 stars per $\text{deg}^2 \text{ mag}^{-1}$ for the selection criteria that we apply.

3.2 Adopted absolute I magnitude of the TRGB

In order to calculate distances to these galaxies, we must adopt a value for the I -band absolute magnitude of the TRGB. We use the most recent observational determination of this position, given by Bellazzini et al. (2001). These authors studied the galactic globular cluster ω Centauri using a very large photometric data base and an independently derived distance estimate to this system which used a detached eclipsing binary star. They derive a value of -4.04 ± 0.12 mag for the I -band magnitude of the TRGB at a metallicity of $[\text{Fe}/\text{H}] \simeq -1.7$ dex, which agrees extremely well with theoretically-derived estimates of this point. Although there is a small variation of this magnitude with metallicity, it is significantly less than the quoted uncertainty for the range of metallicities that we will be considering, given the stellar systems we are analysing. As such, we adopt the value as constant. It is important to note that the uncertainty on this value as it stands would be the single biggest contributor to the uncertainties in our final derived distances, and is approximately four times bigger than our systematic errors. This degree of uncertainty is conservative, and the error quoted is primarily a result of the uncertainty in the true distance modulus of ω Cen, which is of the order of 0.1 mag. We therefore adopt $M_{\text{TRGB}} = -4.04 \pm 0.05$ mag, and note that, although it is possible that the scale may be shifted by up to 0.1 mag, this will affect all of our measurements in the same way. The relative distances, to say M31, will essentially remain unchanged.

3.3 M33

The RGB distribution from the central pointings of our survey of M33 (Ferguson et al., in preparation), located at $1^{\text{h}}33^{\text{m}}50^{\text{s}}.9$, $30^{\circ}39'35''$, is shown in Fig. 3 for all stars brighter than $I = 22.5$ mag in the strip indicated in Fig. 5. The orientations of M33's axes are indicated, as is an elliptical annulus around the edge of the disc, selected so as to avoid the effects of crowding in the inner region while still sampling stars across the entirety of M33's disc. The inner ellipse has a semimajor axis $a = 0.5$, while the outer ellipse has $a = 0.8$. To provide a check that our resulting RGB luminosity function does not suffer heavily from blending effects, we have compared the RGB luminosity functions for elliptical annuli at

¹ See <http://www.ast.cam.ac.uk/~wfcsur/colours.php>.

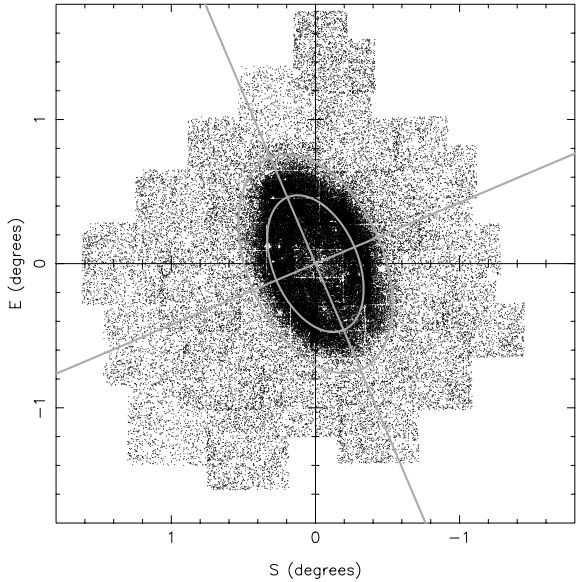


Figure 3. The spatial distribution of RGB stars in M33, from our INT WFC survey of this galaxy (Ferguson et al., in preparation). Only stars brighter than $I = 22.5$ mag lying in the strip indicated in the CMD will be plotted. Stars around the edge of the disc lying in the elliptical annulus will be used in our analysis (0.72 deg^2). The position angle of the disc to the vertical is $\sim 23^\circ$.

different galactocentric radius. The results are shown in Fig. 4 and are all foreground-corrected. The outer annulus samples a region of M33 where we expect negligible crowding, while the innermost annulus might be expected to sample many blended stars. Indeed, the innermost RGB luminosity function is seen to extend to brighter magnitudes than the outermost RGB luminosity function, suggesting that blending may be affecting the inner fields to some extent. In this respect, the middle annulus results in a RGB luminosity function whose overall shape is very similar to the outermost RGB luminosity function, given that the outer RGB luminosity function samples fewer stars and is necessarily more noisy. In fact, the location of the TRGB for the outer annulus is at 20.56 ± 0.02 mag, which compares very well with our final derived value of 20.54 ± 0.01 mag. This implies that the effect of crowding on our M33 data is negligible for $a > 0.5$.

The CMD of the stars we analyse to measure the TRGB is shown in Fig. 5. It is obvious from the width of the RGB that M33 contains a larger spread in age/metallicity than the Andromeda dwarfs (Fig. 8), and the region of the tip lacks a definite edge with many bright AGB stars visible in that region. This is illustrated in the RGB luminosity function (Fig. 6) where we see that the tip of the luminosity function delimits a change in slope rather than an edge, and the AGB stars are also visible here for $I < 20.6$ mag. A weak blue plume representative of a younger stellar population is also evident in the CMD at $V-I \simeq 0$.

A least-squares fit to the RGB LPD gives a TRGB of $I = 20.54 \pm 0.01$ mag. The uncertainty in this measurement is given by the 1σ contour in the $\tau-s$ plane (see Fig. 7). This contour plot was constructed assuming a constant error term in the LPD (Section 2.2). To provide a check of this approximation, we also conduct a similar χ^2 fit to the binned luminosity function, where we know the errors to be well described by a Poisson distribution. The expressions for a and k given by equations (3) and (4) become necessarily more complex, but the contour levels remain nearly unchanged.

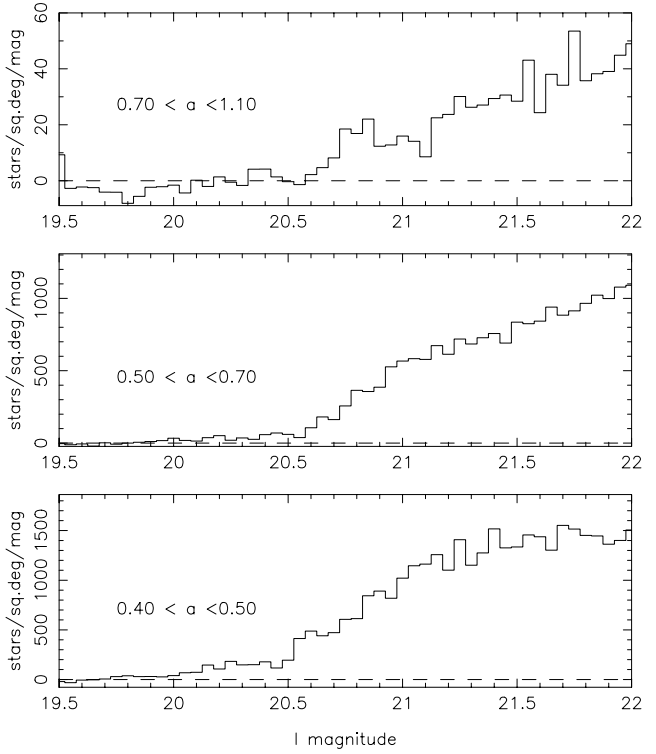


Figure 4. RGB luminosity functions for M33 as a function of galactocentric radius. Each RGB luminosity function is created from stars within elliptical annuli with semimajor axes of a° and have been foreground-corrected. The innermost RGB luminosity function may suffer from stellar blending. However, the similarity of the outer two RGB luminosity functions suggests that blending is having a negligible effect on our TRGB measurement for M33, which uses stars located at $0.5 < a < 0.8$.

From the extinction maps of Schlegel, Finkbeiner & Davis (1998), the interstellar reddening $E(B-V)$ is found to be 0.042 mag, and they state that these values are accurate to within 16 per cent. Using the relation between reddening and extinction in the Landolt system (Landolt 1992), given in the same paper, $A_I = 1.94E(B-V)$, implies that $A_I = 0.081$ mag. We take the absolute I magnitude of the TRGB to be $M_{\text{TRGB}} = -4.04 \pm 0.05$ mag as discussed in Section 3.2. The other uncertainty that we take into account is the mean systematic photometric error in our measurements, which is of the order of 0.02 mag. Blending has already been shown to have a negligible effect on our measurement of the TRGB. Combining the observational errors leads to an overall error of 0.03–0.04 mag in the measured value of the TRGB magnitude. We calculate the distance, D , to the galaxy from $I - M_{\text{TRGB}} = 5\log_{10}D - 5 + A_I$ and conclude that overall, $D_{M33} = 794 \pm 23$ kpc. Application of the heuristic method identifies a tip at 20.6 mag, in good agreement with the more detailed treatment.

This result brings the TRGB distance to M33 into excellent agreement with the Cepheid distances (see Table 1). The suggestion of a significant amount of reddening in M33 by Kim et al. (2002), to explain the discrepancy between their TRGB measurements and their Cepheid measurements (Lee et al. 2002), seems unlikely. We attribute the difference in our results to the fact that we have better statistics than was possible to achieve with their smaller *HST* fields—we do not see evidence for a significant jump at ~ 20.9 mag, as these authors do (see their fig. 4). Of the 10 fields that they analyse, several of the luminosity functions do show evidence for a discontinuity

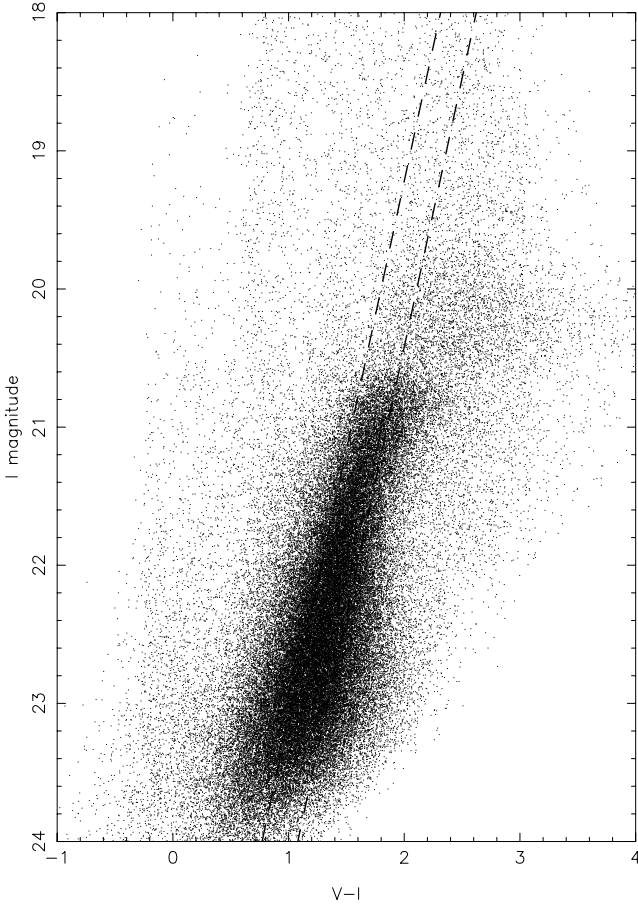


Figure 5. The CMD of the spiral galaxy M33, using stars in the elliptical annulus shown in Fig. 3. A bright AGB star population is obvious above the TRGB. Only stars in the strip indicated were used in the construction of the luminosity function. Selecting such a narrow strip along the RGB still gives us ample stars for our analysis and significantly decreases the AGB contamination.

in the slope at $\sim 20.5\text{--}20.6$ mag, which may well be associated with the discontinuity that we attribute as the TRGB in our luminosity function. Because our algorithm defines the location of the TRGB differently to an edge detection algorithm, then this location is highlighted in preference to any absolute change in counts. Additionally, it is unlikely that we have instead measured a feature due to AGB contamination – an AGB population is clearly observed in the CMD and RGB luminosity function for this galaxy (Figs 5 and 6) and so there would have to be a second AGB population in the CMD exactly coincident with the top of the RGB, although this seems unlikely. We would also expect that, if this was the case, their effect would be lessened in a luminosity function located at larger galactocentric distance. Inspection of Fig. 4 shows that this is not the case for these stars, even though the contribution from the known AGB component can be seen to reduce in the expected way.

Kim et al. have also calculated the distance to M33 using the red clump (RC), finding agreement with their TRGB measurement. This feature represents stars with a helium core and a hydrogen shell passing through a relatively slow phase of their luminosity evolution, leading to a clump appearing in the CMD. They have recently been suggested for use as a distance indicator by Paczynski & Stanek (1998). They compared the I -band magnitude of OGLE RC stars seen through Baade's window with a sample from the

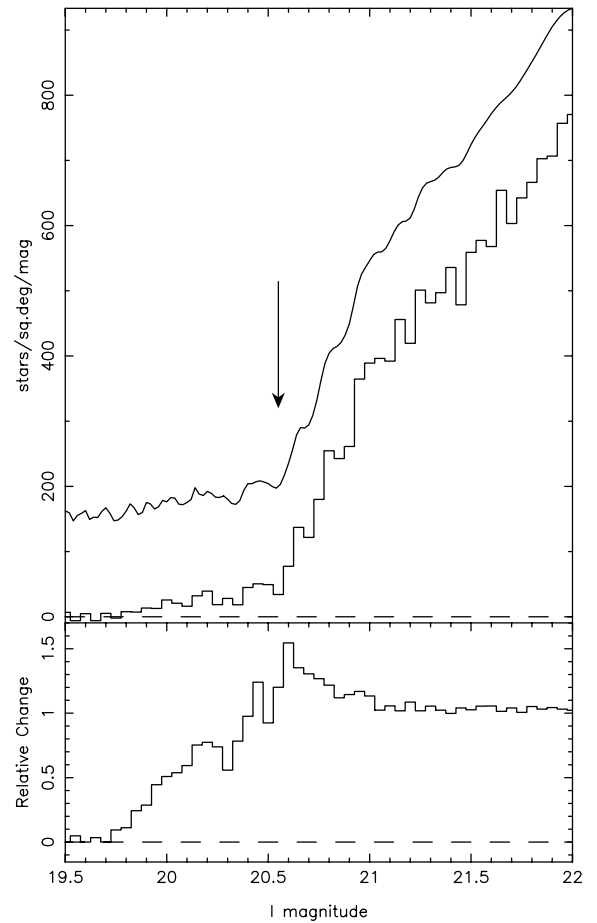


Figure 6. Upper panel: The RGB luminosity function for M33 (lower curve is binned luminosity function, upper curve is offset LPD) with an arrow indicating the measured position of the TRGB using the fit of an adaptive slope. This location is partially masked by an AGB population, although its determination is still possible by use of the least-squares method. The area of sky used in this analysis is the area contained by the elliptical annulus shown in Fig. 3. Lower panel: The TRGB as identified by the heuristic method.

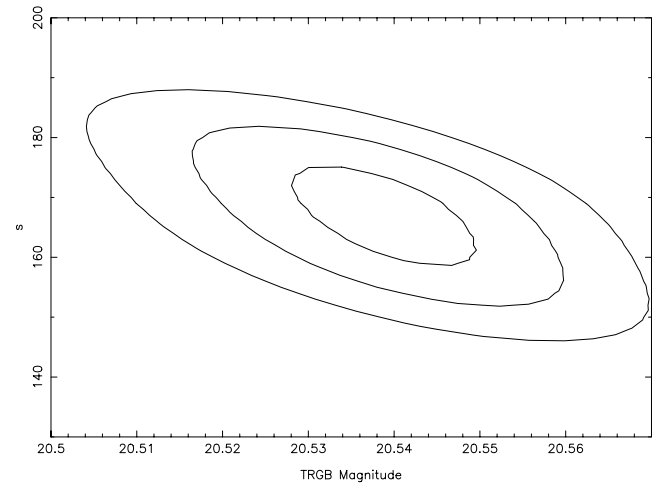


Figure 7. Contour plot of the measured TRGB location versus the slope parameter, s , for M33. Contours show the 1σ , 2σ and 3σ confidence levels.

Table 1. The distance to M33, along with a selection of the most recent distance estimates to M33 based on *HST* data.

$(m-M)_0$	Distance	Method	Reference
24.50 ± 0.06	794 ± 23 kpc	TRGB	This study
24.52 ± 0.14	802 ± 51 kpc	Cepheids	Lee et al. (2002)
24.81 ± 0.13	916 ± 55 kpc	TRGB	Kim et al. (2002)
24.80 ± 0.14	912 ± 59 kpc	RC	Kim et al. (2002)

Hipparcos catalogue with parallaxes known to ≤ 10 per cent, allowing the absolute I magnitude of the RC (M_I^{RC}), and hence a distance, to be calculated for the stars seen towards the Galactic Centre. The reliability of this method when applied to other stellar systems relies on the similarity of the *Hipparcos* sample with the RC stars in the system of interest, and remains a controversial point because of possible dependences of M_I^{RC} on the properties of the population. Theoretical models seem to predict a relatively strong dependency of M_I^{RC} with age and metallicity (e.g. Cole 1998; Girardi et al. 1998; Girardi 2000; Girardi & Salaris 2001) while observational studies are in apparent disagreement with each other (e.g. Udalski 1998; Sarajedini 1999). However, both observation and theory show that M_I^{RC} is significantly fainter for stars with ages > 10 Gyr than for their intermediate age counterparts (Udalski 1998; Girardi & Salaris 2001). Kim et al. (2002) assume that the majority of the stellar population in M33 is old (> 10 Gyr) in order to associate the mean metallicity of the RGB with the metallicity of the RC. This

metallicity is then used to calculate M_I^{RC} using the calibrations for M_I^{RC} versus [Fe/H] by Udalski (1998) and Popowski (2000). However, it is not clear that these calibrations are valid for M33 given the assumption about the age of the bulk of the stellar population. If M_I^{RC} is significantly fainter in this galaxy because of age, then M33 will be correspondingly closer than these authors calculated.

3.4 Andromeda I

The dwarf spheroidal galaxy And I was discovered by van den Bergh (1971) and lies at $0^h45^m39.8^\circ, 38^\circ2'28''$. It is a satellite galaxy of M31 at a projected distance of ~ 40 kpc. Mould & Kristian (1990) were the first to study its RGB using CCD images taken at the prime focus of the Hale telescope. Using an eyeball determination of the TRGB, they found it to be at a distance of 790 ± 60 kpc. They also concluded the galaxy to be of intermediate metallicity. Da Costa et al. (1996) obtained *HST* WFPC2 images of this system and, by comparison with the giant branches of several globular clusters, confirmed the metallicity to be $\langle [\text{Fe}/\text{H}] \rangle = -1.45 \pm 0.2$ dex. By analysing the morphology of the horizontal branch, they also came to the conclusion that the majority of the population is approximately 10 Gyr old. However, the presence of a blue horizontal branch and RR Lyrae stars shows that there is a minority population at least 3 Gyr older than this. And I, like many other dwarf spheroidals, appears to have undergone an extended period of star formation.

The CMD for And I is shown in the left panel of Fig. 8. The upper few magnitudes of the RGB are clearly observed and even by visual

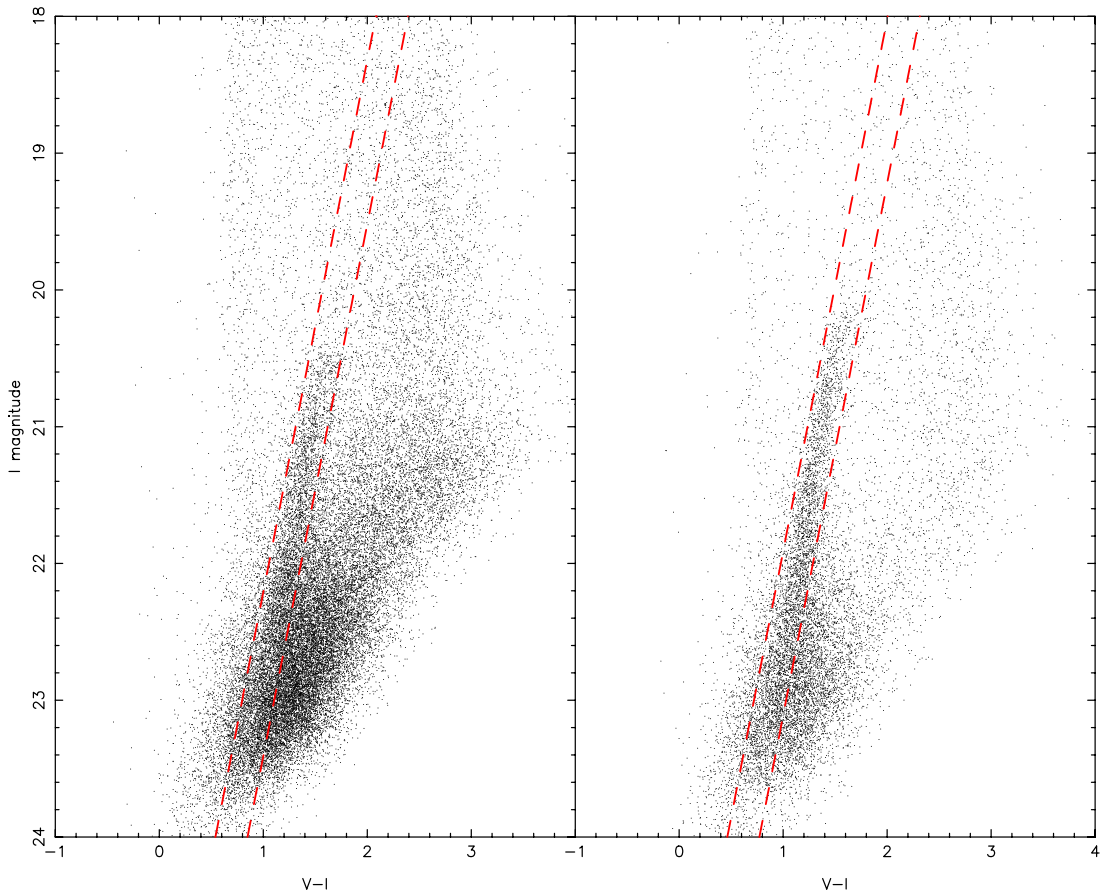


Figure 8. The CMDs for the dwarf galaxies And I (left panel) and And II (right panel). The luminosity function is constructed from the region contained within the dotted lines. The RGB is easily visible in both cases with the tip at $I \simeq 20.45$ mag for And I and $I \simeq 20.1$ mag for And II. The additional red component centred around $V-I \simeq 2.4$ in the left panel is a result of the giant Andromeda tidal stream discovered by our INT survey of M31 (Ibata et al. 2001; Ferguson et al. 2002; McConnachie et al. 2003) which extends over the region around And I.

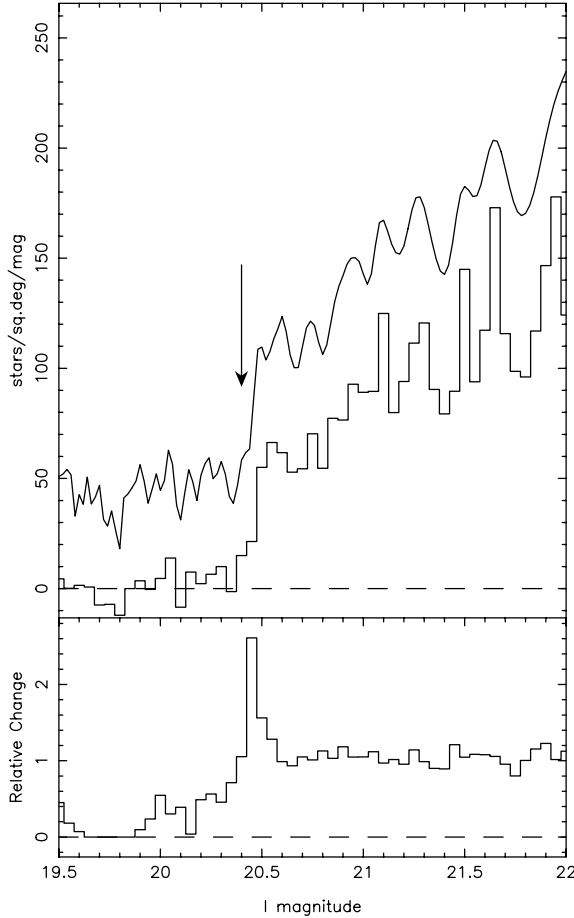


Figure 9. Upper panel: The solid line shows the (RGB) luminosity function of And I. The dashed line shows the (RGB) LPD. The total area of sky surveyed was 0.47 deg^2 . The arrow indicates the position that we measure the TRGB to be located using our adaptive slope. Lower panel: Measurement of the location of the tip using the heuristic method, showing excellent agreement with the adaptive slope.

inspection we can determine that the tip is at $I \simeq 20.45$ mag. One interesting point of note is the additional red feature ($V-I > 2$) that is not present in the And II CMD (right panel). This is because of the giant stellar stream first discovered by our survey of the outer regions of M31, which is sufficiently broad that part of it lies along the line of sight to And I.

Application of the least-squares method identifies the TRGB to be at $I = 20.40^{+0.03}_{-0.02}$ mag, as shown in Fig. 9. Schlegel et al. (1998) give $E(B-V) = 0.056$ mag for the interstellar reddening, and so we derive $D_{\text{AndI}} = 735 \pm 23$ kpc, closer than had previously been determined (Table 2) but still in reasonable agreement. Application of the heuristic method identifies the tip to lie at 20.45 mag (Fig. 9), in excellent agreement with the adaptive slope, not unexpected for such a clean LPD.

Table 2. The distance to And I, together with previous estimates.

$(m-M)_0$	Distance	Method	Reference
24.33 ± 0.07	735 ± 23 kpc	TRGB	This study
24.50 ± 0.15	790 ± 60 kpc	TRGB	Mould & Kristian (1990)
24.55 ± 0.08	810 ± 30 kpc	Horizontal branch stars	Da Costa et al. (1996)

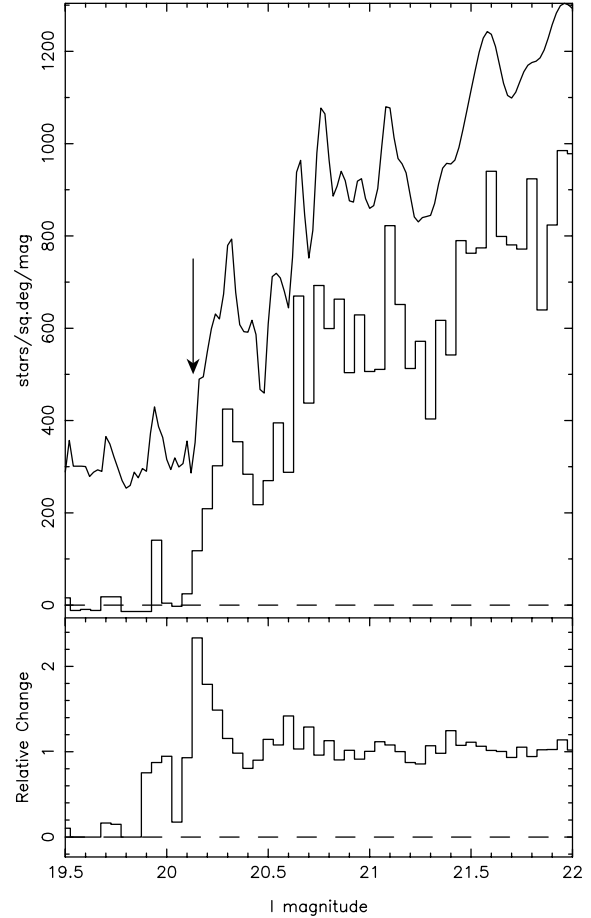


Figure 10. Same as Fig. 9, but for the dwarf galaxy And II. This shows all stars located within 0.1 of the centre of this galaxy, allowing the rest of the field to be used as a local foreground correction.

Table 3. The distance to And II, together with previous estimates.

$(m-M)_0$	Distance	Method	Reference
24.05 ± 0.06	645 ± 19 kpc	TRGB	This study
$23.83^{+0.46}_{-0.38}$	583^{+124}_{-103} kpc	Giant branch fitting	Koenig et al. (1993)
24.17 ± 0.06	680 ± 20 kpc	Horizontal branch stars	Da Costa et al. (2000)

3.5 Andromeda II

And II is another dwarf spheroidal satellite of M31 discovered at the same time as And I. It lies at $1^h 16^m 29.8^s, 33^\circ 25' 9''$, approximately 140 kpc in projection from M31, towards M33. Despite the fact that it lies significantly closer to M33 in projection, the larger mass of M31 means that it is most likely a satellite of M31. Da Costa et al. (2000) derive a mean metallicity of $\langle [\text{Fe}/\text{H}] \rangle = -1.49 \pm 0.11$ dex with a significantly larger abundance spread than in And I. An old (≥ 10 Gyr) population is again implied from the presence of a blue horizontal branch. The presence of young or intermediate populations in this galaxy remains a possibility from their study, but we detect no sign of such a population to $M_V \simeq 0$ mag.

The CMD for And II (right panel of Fig. 8) again shows the upper parts of the RGB very clearly, with a tip visible at $I \simeq 20.1$ mag. We construct the luminosity function for And II by using stars within 0.1 from its centre. This then allows us to apply a local foreground

correction to the luminosity function by using as a reference population all stars on the same INT field outside this radius, scaled in the usual way. The result is shown in Fig. 10, where an unambiguous tip can be observed. We find the TRGB to lie at 20.13 ± 0.02 mag (20.15 mag using the heuristic technique). From Schlegel et al. (1998), $E(B-V) = 0.063$ mag. This corresponds to $D_{\text{And II}} = 645 \pm 19$ kpc, in reasonable agreement with estimates that have been made using other methods (Table 3).

4 SUMMARY

In this paper we have introduced a new quantitative method for the determination of distances to metal-poor stellar systems using the TRGB as a standard candle, accurate to typically ± 0.02 mag rms, ± 0.03 mag systematic. The method involves a least-squares fit of a data adaptive slope template to the foreground-corrected RGB LPD in 1-mag windows, to find the region of the LPD that is best fit as a simple slope function, i.e. the region that shows the most significant decline in counts as we go to brighter magnitudes. This determines the apparent magnitude of the TRGB, as represented in the luminosity function. Observations and stellar evolutionary codes agree that this magnitude is virtually constant for old, metal-poor populations, and so the photometric parallax can easily be calculated.

We believe that our method provides significant improvements over previous attempts to locate the TRGB in a luminosity function. By only considering stars along a strip in the CMD, we minimize contamination from other stellar populations. Further, for systems with broader RGBs we ensure that our sample of RGB stars all have similar age/metallicity rather than analysing all the stars in the RGB. Poisson noise will affect us to a much smaller degree than previous methods because we consider a range in magnitude when determining the position of the tip, rather than just comparing neighbouring star counts. Tests of our method on both synthetic and real data demonstrate the robustness of this method, even with relatively poor S/N. Perhaps most importantly, we demonstrate that accurate TRGB determinations require the use of Wide Field Cameras, such as that on the INT, in order to boost star counts and allow the measured RGB to be as accurate and complete a representation of the population as possible.

The methodology that we develop in this paper is applied to three galaxies: And I & II, and M33. We derive distances to these objects of 735 ± 23 , 645 ± 19 and 794 ± 23 kpc, respectively (see Tables 1, 2 and 3 for comparison with previous results). The contribution to this uncertainty due to the algorithm is only of the order of 15 kpc, demonstrating a significant improvement over other previous techniques that have been used. What is perhaps of greatest importance when comparing this algorithm with, for example, the edge detection algorithm of Sakai et al. (1996) or the maximum likelihood method of Mendez et al. (2002), is that it uses a different set of criteria to define the location of the tip. In the majority of situations, where the tip position is marked by a significant jump in star counts, the methods will be expected to give the same result. In other situations (such as a gradual increase in star counts at the TRGB edge, nicely demonstrated in M33) we would not necessarily expect the algorithms to agree as they search for fundamentally different features in the luminosity function. In the second paper in this series (McConnachie et al. 2004) we apply our algorithm to 11 other Local Group galaxies – And III, And V, And VI, And VII, NGC 185, NGC 147, Pegasus, WLM, LGS3, Cetus and Aquarius – to create a homogeneous set of distances to nearby galaxies, a majority of which are members of the M31 subgroup.

ACKNOWLEDGMENTS

Many thanks to the referee, Barry Madore, for a careful reading of this manuscript and useful comments. Additionally, we would like to thank Minsun Kim and collaborators for supplying us with their M33 *HST/WFPC2* data, and Eline Tolstoy for her opinion on some of the arguments presented in this paper. The research of AMNF has been supported by a Marie Curie Fellowship of the European Community under contract number HPMF-CT-2002-01758.

REFERENCES

- Bellazzini M., Ferraro F. R., Pancino E., 2001, ApJ, 556, 635
 Cole A. A., 1998, ApJ, 500, L137
 Crocker D. A., Rood R. T., 1984, Proc. IAU Symp. 105. Kluwer, Dordrecht, p. 159
 Da Costa G. S., Armandroff T. E., 1990, AJ, 100, 162
 Da Costa G. S., Armandroff T. E., Caldwell N., Seitzer P., 1996, AJ, 112, 6
 Da Costa G. S., Armandroff T. E., Caldwell N., Seitzer P., 2000, AJ, 119, 705
 Ferguson A. M. N., Irwin M., Ibata R., Lewis G., Tanvir N., 2002, AJ, 124, 1452
 Girardi L., 2000, Highlights Astron., 12
 Girardi L., Salaris M., 2001, MNRAS, 323, 109
 Girardi L., Groenewegen M. A. T., Weiss A., Salaris M., 1998, MNRAS, 301, 149
 Harris W. E., Durrell P. R., Pierce M. J., Secker J., 1998, Nat, 395, 45
 Ibata R., Irwin M., Lewis G., Ferguson A. M. N., Tanvir N., 2001, Nat, 412, 49
 Iben I. J., Renzini A., 1983, ARA&A, 21, 271
 Irwin M., Lewis J., 2001, NewARev., 45, 105
 Kim M., Kim E., Lee M. G., Sarajedini A., Geisler D., 2002, AJ, 123, 244
 Koenig C. B. H., Nemec J. M., Mould J. R., Fahlman G. G., 1993, AJ, 106, 1819
 Landolt A. U., 1992, AJ, 104, 340L
 Lee M. G., Freedman W. L., Madore B. F., 1993, ApJ, 417, 553
 Lee M. G., Kim M., Sarajedini A., Geisler D., Gieren W., 2002, ApJ, 565, 959
 McConnachie A. W., Irwin M. J., Ibata R. A., Ferguson A. M. N., Lewis G. F., Tanvir N., 2003, MNRAS, 343, 1335
 McConnachie A. W., Irwin M. J., Ibata R. A., Ferguson A. M. N., Lewis G. F., Tanvir N., 2004, MNRAS, submitted
 Madore B. F., Freedman W. L., 1995, AJ, 109, 1645
 Maíz-Apellániz J., Cieza L., MacKenty J. W., 2002, AJ, 123, 1307
 Mendez B., Davis M., Moustakas J., Newman J., Madore B. F., Freedman W. L., 2002, AJ, 124, 213
 Mould J., Kristian J., 1990, ApJ, 354, 438
 Popowski P., 2000, ApJ, 528, L9
 Paczynski B., Stanek K. Z., 1998, ApJ, 494, L219
 Sakai S., Madore B. F., Freedman W. L., 1996, ApJ, 461, 713
 Salaris M., Cassisi S., 1997, MNRAS, 289, 406
 Sarajedini A., 1999, AJ, 118, 2321
 Schlegel D. J., Finkbeiner D. P., Davis M., 1998, AJ, 500, 525
 Tanvir N., 1999, in Egret D., Heck A., eds, ASP Conf. Ser. 167. Astron. Soc. Pac., San Francisco, p. 84
 Udalski A., 1998, Acta Astron., 48, 383
 van den Bergh S., 1971, ApJ, 171, L31
 Walton N. A., Lennon D. J., Greimel R., Irwin M., Lewis J., Rixon G. T., 2001, ING Newslett., No. 4, 7
 Zoccali M., Piotto G., 2000, A&A, 358, 943